Structure of Thunderstorm Gust Fronts with Topographic Effects

A. A. Bidokhti and T. Bani-Hashem

Institute of Geophysics, Tehran University, P.O. Box 14155-6466, Tehran, I.R. Iran

(Received January 9, 2001; revised June 6, 2001)

ABSTRACT

Surface meteorological observations, associated with gust fronts produced by thunderstorm outflows over Tehran, an area surrounded by mountains, have been analyzed. Distinctive features are sudden drop in air temperature, up to 10°C, sharp increase in wind speed, up to 30 m s^{-1}, with wind shift, to northwesterly, pressure jump, up to 4 hPa, humidity increase, up to 40%, and rain after some 20 min. Gust fronts which often occur in spring time, have a typical thickness of about 1.5 km and produce vertical wind shear of the order of $10^{-2}s^{-1}$. Although these features seem to be common for most of the events, their intensities differ from one event to another, indicating that the gust fronts may occur in different sizes and shapes. Apart from a dominant effect on the formation of the original thunderstorms, topography appears to break up the frontal structure of the gust fronts. The internal Rossby radius of deformation for these flows is small enough (~ 100 km) for rotational effects to be minor.

A laboratory model of the gust front (gravity current) also shows that it initially has a distinctive head with a turbulent wake, and can be broken up by topography. It is shown that when the environment is stratified, turbulence due to lobes and clefts instabilities near the nose of the current is suppressed. When the ground is rough, these instabilities are highly amplified and the internal Froude number of the flow is reduced. The bottom slope in the presence of rough topography leads to the break up of the current head and produces a broad and highly non-uniform head, recognized in the density signals.

Key words: Frontal structure, Gravity current, Meteorological data, Outflows

1. Introduction

Gust fronts are formed as a result of surface spreading of cold air downdraft from severe thunderstorms. The downdraft itself is originated by precipitation drag and evaporative cooling of the rain, and, once it reaches the ground, it spreads out and lifts up the lighter, warmer surface air which can generate another thunderstorm and so on.

Gust front studies not only are of considerable interest in meteorology in general (as they are some manifestations of intensive vertical energy exchange in troposphere), but also, because of producing near surface changes in the atmospheric boundary layer, in air pollution and aviation, in particular (e.g., Wakimoto, 1982; Bowen, 1996; Manasseh and Middleton, 1995). Goff (1976) studied gust fronts, using tower data, and found four stages in their life cycle. Wakimoto (1982) also found the same stages, using radar data. Gust fronts may set off atmospheric bore and oscillations, if there is a near-surface inversion (Manasseh, and Middleton, 1995). The surface inversion, produced by some precedent gust fronts, also leads to suppression of turbulence in the surface layer (Bowen, 1996). Gust fronts in desert areas can take up dust and appear as gigantic structures of dust storms, which can dramatically change visibility (Simpson, 1986).

The structure of gust fronts is very similar to that of gravity currents with a circulating vortex like head and a turbulent wake, with a depth of less than that of the head. The Kelvin–Helmholtz (K–H) instability near the top surface of the outflow has been considered as the main cause of the turbulence (Mahoney, 1988; Wechwerth and Wakimoto, 1992).

The aim of this work is a further study on the structure of the gust fronts in a mountainous area, using surface meteorological data and some physical modeling in the laboratory.

2. Data and analysis

The surface meteorological data used in this study have mainly been obtained from three land stations, Shemiran, Institute of Geophysics and Mehrabad, 10 km apart approximately, and, elevated at 1485 m, 1423 m and 1191 m above mean sea level, respectively. The stations are located about north of Tehran, south of a nearly east–west mountain range, with an average elevation of 3500 m (Fig. 1). The automatic data recording systems are equipped with surface meteorological sensors of wind, air temperature, pressure, himidity and precipitation.

Some 200 gust fronts have been observed, mainly during 1990–1993 and a few cases with more details during 1995–1997. Some gust fronts from Kerman and Ahwaz areas, which are in the southern part of Iran, have also been studied.

Overall, observations show that the gust fronts often occur in the afternoons of spring or early summer days, as the convective instability is strong enough for the thunderstorm formation. The northern mountain seems to play a profound key role in forcing the vertical uplift and thunderstorm genesis, in agreement with the mechanism proposed by Banta and Schaaf

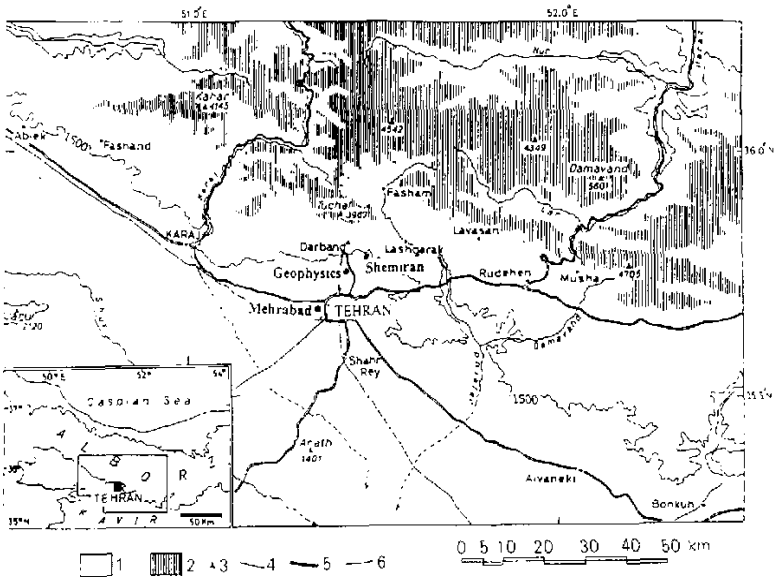

Fig. 1. A map of Tehran area for gust front observations: 1: area north of 1500 m ASL contour; 2: area higher than 3000 m; 3: height point; 4: river; 5: road; 6: rail; observation points: Mehrabad, Geophysics, Shemiran.

(1986).

Synoptic features often associated with the periods of thunderstorm activities, are a deep trough over Turkey and Mediterranean Sea on 500-hPa level, a thermal low over Arabian Peninsula and a south westerly jet stream on 300-hPa level over the western part of Iran.

It is sometimes observed (Fig. 2) that a secondary gust front after the primary one is set up, that moves in the opposite direction. This may be due to the thunderstorm formation, which is excited by the primary gust front, downstream of the observational point.

Figure 3 shows records of a typical gust front at Geophysics station. The wind speed, after a prefrontal small drop, has a sudden jump with a turbulent wake. The wind direction often rotates clockwise, becoming north westerly (Fig. 4). Figure 5 shows the wind speed record of Fig. 4 and indicates that as the gust front enters urban rough area (Mehrabad and Shemiran) it is dissipated substantially. The drop in temperature is rather sharp, up to 10°C within a period of 15 minutes. The perssure increase is up to 4 hPa within half an hour, due to the hydrostatic effect. Duration of the gust fronts, passing the station, on the average is about 25 minutes. They appear in different sizes and shapes. Figure 6 shows, for example, time series of two different types of which one has a well-defined characteristic of gravity currents and another is less typical and probably broken off by topographic effects.

Such behavior is also observed in laboratory models with topographic effect. The multiple gust fronts of the type Fig. 4b are often observed which could be related to either topographic effects (with peaks close together) or thunderstorm pulsations (Goff, 1976).

Table 1 gives the mean values for the Froude number Fr; depth, h; the gust front speed, u; the maximum speed, u_{max}; and the ratio u_{max}/u, based on the data obtained from various case studies at different geographical locations, including mainly Tehran (154 cases), Kerman (44 cases) and Ahwaz (17 cases) areas, depending on availability of good data, with

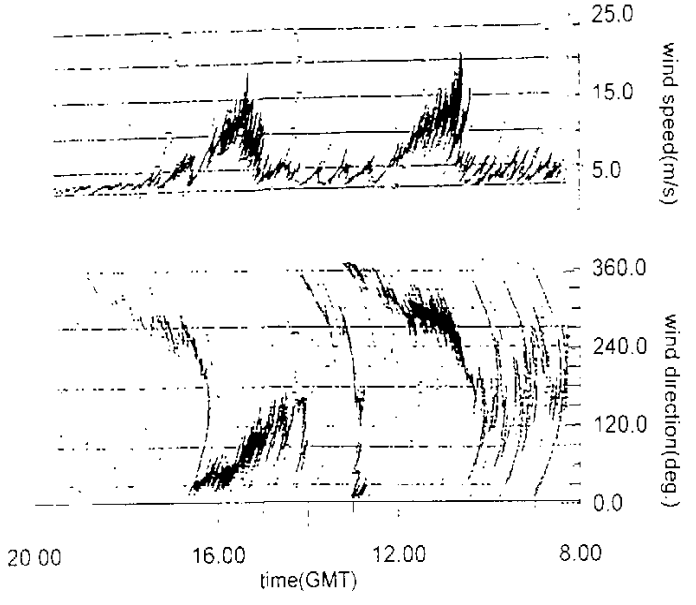

Fig. 2. An example of wind record of a gust front at Geophysics for 24 / 5 / 91. Notice that the second front may be due to the thunderstorm in the east that may have been excited by the first gust front.

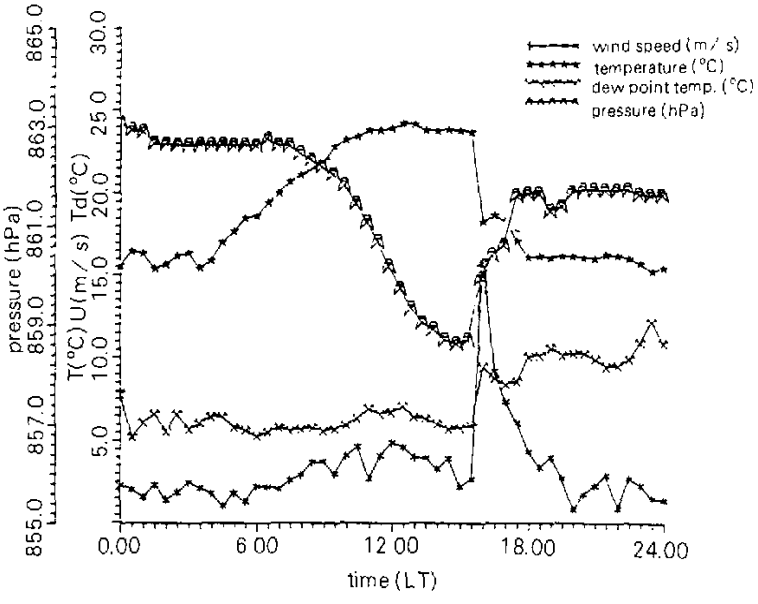

Fig. 3. Graphs of temperature, wet-bulb temperature, wind speed and pressure during the event of 27th May, 1995. The time of occurrence is about 6:00 pm, LT (Geophysics).

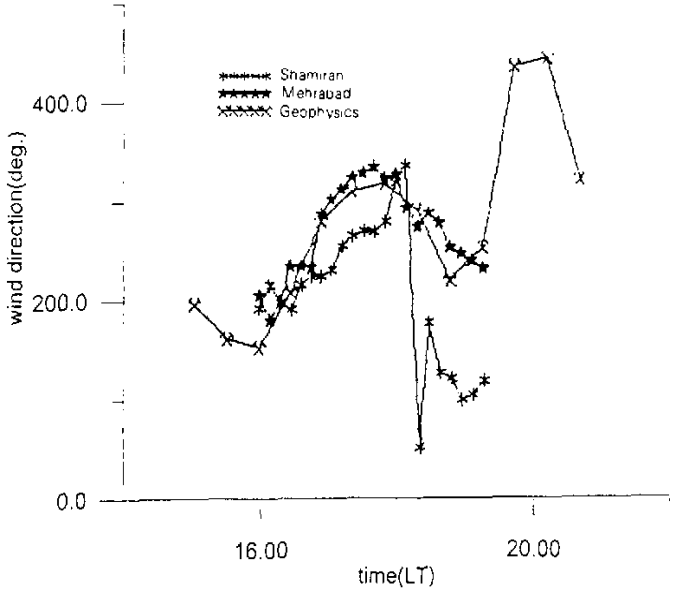

Fig. 4. Same as Fig. 3, but of wind direction and for three Tehran stations.

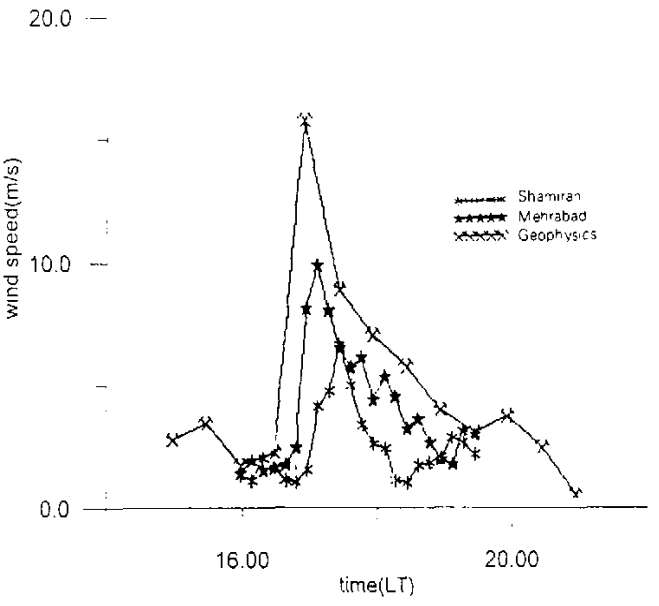

Fig. 5. Same as Fig. 4, but for wind speed.

somewhat different climates, where details of the cases are given in Rangbar (1997). These observations agree well with those of other investigators (e.g. Wakimoto, 1982; Goff, 1976; Mahoney, 1988). Hence, it seems that the gust fronts, mainly of the American plain, are quite similar in behavior and structure to those studied here. The discrepancies in the figures, particularly in the value of the Froude number (Table 1), may be due to the orography and the distance from the thunderstorm, generating the gust fronts. It is known that when the environment is stratified, the motion of the gust front is associated with internal waves and Fr is reduced (Simpson, 1986). Tehran area is more mountainous than Kerman and Ahwaz areas. This may indicate that rough terrain may reduce gust front speed and its Fr, although the local climate and atmospheric boundary layer may be important in their characteristics.

Table 1. Mean values of some observed or calculated gust fronts' parameters

Station	Tehran (154 cases)	Kerman (44 cases)	Ahwaz (17 cases)
Mean parameters			
Speed $\bar{u}$(m / s)	10.8	9.0	9.4
Thickness $\bar{h}$(km)	1.55	0.78	1.32
Max speed $\bar{u}_{max}$ (m / s)	15.7	13.4	12.6
Froude number $\bar{Fr}$	0.97	1.26	0.77
Speed ratio $\bar{u}_{max} / \bar{u}$	1.45	1.49	1.34

3. The dynamics and structure of the gust fronts

Dynamically, the gust fronts are similar to the gravity currents produced in the laboratory (Simpson, 1986). Detailed observations of the gust fronts, however, show that they may have other features, such as internal gravity waves, and K–H waves due to the cross-shear on their upper boundary (Weckwerth and Wakimoto, 1992). These effects can cause nonhomogeneity along the gust fronts, which has been assumed homogeneous previously (Wakimoto, 1982).

Due to this similarity, one can assume an expression for the speed of the leading edge of the gust front, u, on a horizontal surface as

$$u = k[g\frac{\Delta\rho}{\rho}h]^{1/2} = k(\frac{\Delta P}{\rho})^{1/2}, \tag{1}$$

where k is a kind of Froude number, varying between 0.8–1.4 (Wakimoto, 1982). $\Delta\rho$ is the density difference between cold-air outflow and environment, ρ is the average density of air and ΔP is the hydrostatic pressure rise.

For a gravity current on an inclined boundary with a slope angle of 5° to 90°, the flow behaves as an inclined negatively buoyant thermal (Beghin, et al., 1981). This is associated with an accelerating phase, followed by a decelerating phase, with a speed of

$$u = K(g\frac{\Delta\rho}{\rho}Q_0)^{1/2} \propto x^{-1/2}, \tag{2}$$

where $K = c\sin^{1/2}\theta$, Q_0 is the volume of the thermal per unit width, θ is the slope angle of the boundary, and c is a shape factor which also depends on the entrainment coefficient, and x is the distance travelled. Typical values of K, dependent on θ in the range of 10° to 20°, are of the order of 2.4 (Beghin, et al., 1981). For a terrain, with a slop of 5°, the current behaves like a gravity current. The reduction in u with x is mainly due to the increase in entrainment and mixing.

The nonhydrostatic pressure change at the nose of the head of the current, when the ambient air is almost stagnant, is about $(1/2)\rho u^2$ according to the Bernoulli theorem. This pressure increase can cause a reduction in the speed of the undisturbed flow before the arrival of the front. Such reduction has been observed occasionally in the present observations (e.g. Figure 1). In fact, often a two-stage pressure rise is observed, where the first stage is probably of a nondydrostatic nature.

The gust front may be considered as a two-dimensional phenomenon (Wakimoto, 1982), where the density variation with height is not significant. Hence, the continuity equation can be used to estimate the vertical wind speed at the head of the front as follows:

$$w = \int_0^h \frac{1}{u}\frac{\partial u}{\partial t}dz, \tag{3}$$

where h is the depth of the head.

Some gust fronts have secondary surges, which are often observed to be irregular and may be due to the thunderstorm activity variations or topography effect that the latter can reflect or break up the current head as they collide with mountains. The increase in surface roughness (such as urban area) can also enhance the dissipation of the fronts. Figure 5 for example shows that as gust front passes part of the city of Tehran, its speed is reduced by more

than 50%.

4. Physical simulation

Gust fronts have a Froude number, $Fr = u / (g'h)^{1/2}$, where $g' = (\Delta\rho / \rho)g$, similar to the Fr of laboratory gravity currents, of the order of unity. On the other hand, the Reynolds number, Re, of the two flows is different, but being both much larger than 500, making them Re independent (Simpson, 1986). Typical Re for gust fronts is 10^8 but for the laboratory gravity currents, here is 10^4. For gravity currents Fr is also dependent on h/H where h and H are current and main fluid depth respectively. For currents with friction and mixing, where h/H varies between 0.05 to 0.3, the corresponding Fr varies almost linearly between 1.3 to 0.7 (Simpson, 1986). h/H for these simulation is about 0.3 but for gust front $h/H \sim 0.2$ (where H is the depth of troposphere).

As the gust fronts occur on different topographies, three types of experiments have been carried out, a-cases with horizontal bottom surface without bottom topography; b-cases with horizontal bottom surface but with bottom topography; c-cases in which the bottom surface has topographic effect as well as not being horizontal.

The experiments were carried out in a long water channel, 30 × 25 cm cross-section and 300 cm long, closed at one end by a gate, which is, filled with a saline solution, with an equivalent density difference of gust front cold air, typically $\Delta\rho / \rho \approx 0.03$ and $u \approx 10$ cm / s (Fig. 7). The gate is withdrawn and the current, following an accelerating phase, moves along the bottom of the tank. Two fast response salinity probes and a computer recorded the passage of the current with a sampling time of (1 / 40) sec. and flow visualization revealed the speed and the structure of the current.

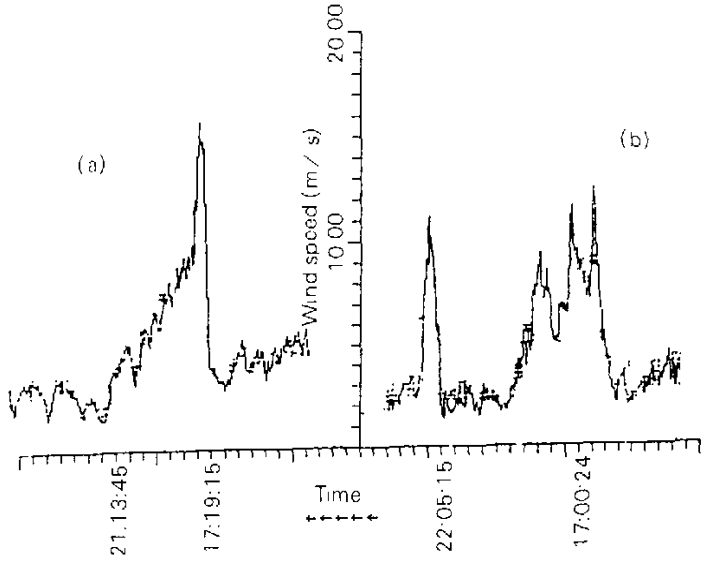

Fig. 6. Wind speed during the passage of gust fronts, (a) without and (b) with topographic effect (Geophysics).

In the first case, the gravity current consists of a thick head with an internal circulation. At the top and behind the head, there is an intense mixing as a result of Kelvin–Helmholtz instability (K–H). The K–H rolls, as noticed in thunderstorm observations (e.g. Muller and Carbone, 1986), may appear as vortex tubes parallel to the top surface. These rolls may be responsible for rather regular large peaks (after the main peak which is due to the head) in the density signal of the experiments (Fig. 8) or velocity signal of the real gust fronts (Fig. 6a).

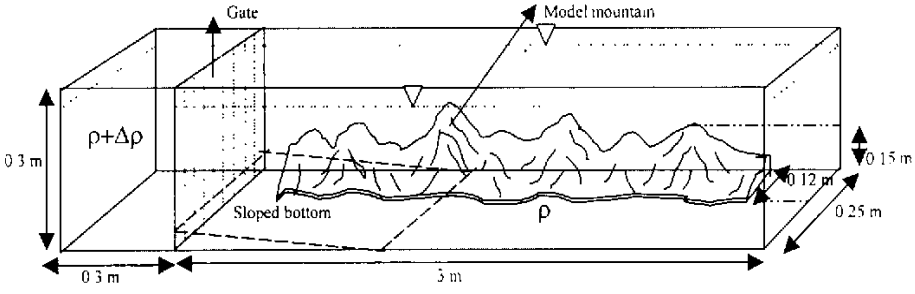

Fig. 7. Experimental set–up.

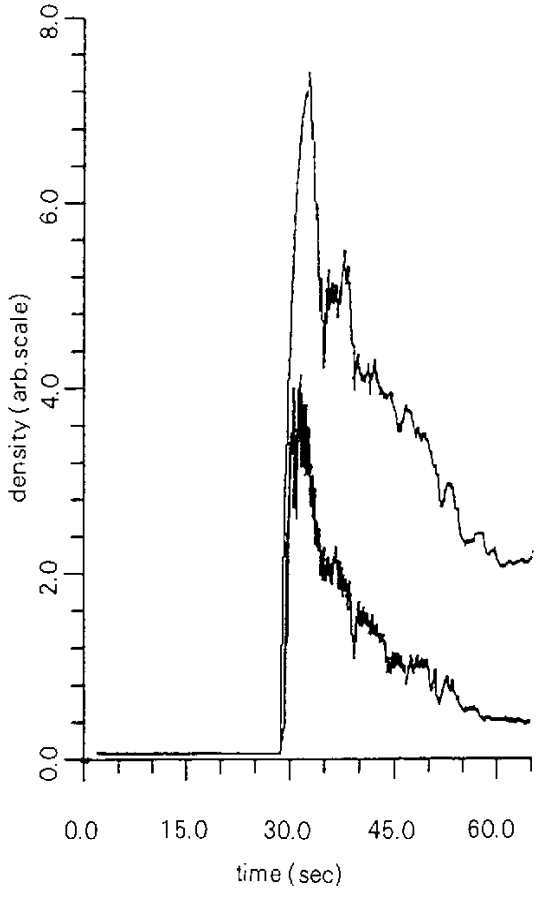

Fig. 8. Salinity signals, without topography, sloped bottom surface and stratification. The upper signal is from the probe near the floor and the lower from the one 5 cm above the floor ($Fr = 0.9$).

The signals in Fig. 8 are from the two density probes, one of which is placed near the bottom and the other 5 cm above it. Fr in this case is about 0.9.

Figure 9 shows a similar case but with a stratified layer near the bottom (formed after a precedent current). Notice the reduction of fine scale turbulence (due to lobes and cliffs instabilities in non-stratified case, e.g. Simpson, 1986) in the signal. However, this stability seems to have little effect on billow formation due to K–H instability. However, it has been shown that when the interface thickness between the current and the ambient fluid, or the ratio of interface thickness to current depth increases, even K–H billows are reduced (Britter and Simpson, 1981).

In the second set of experiments, a rough topography (similar to the side of the northern mountain range of Tehran) was placed along one side of the bottom of the channel, with a smooth transition from the open channel to the full mountain shape obstacle. The height of obstacle was about 10 cm near the wall of the channel, and gradually reduced to zero near the middle of the channel.

The salinity signals (Fig. 10) show that the effect of topography is to broaden the head of the gravity current and produce stronger peaks behind the main broad head. The effect of near bottom stability, is again a reduction of the small scale turbulence associated with

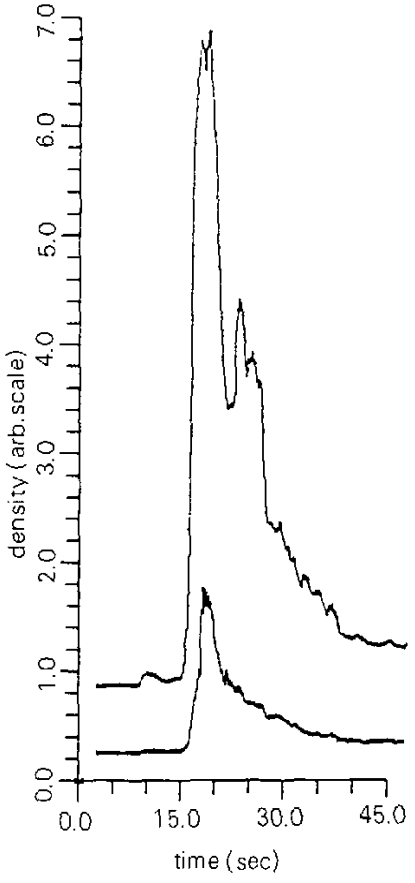

Fig. 9. Same as Fig. 8, but with stratification ($Fr = 0.85$).

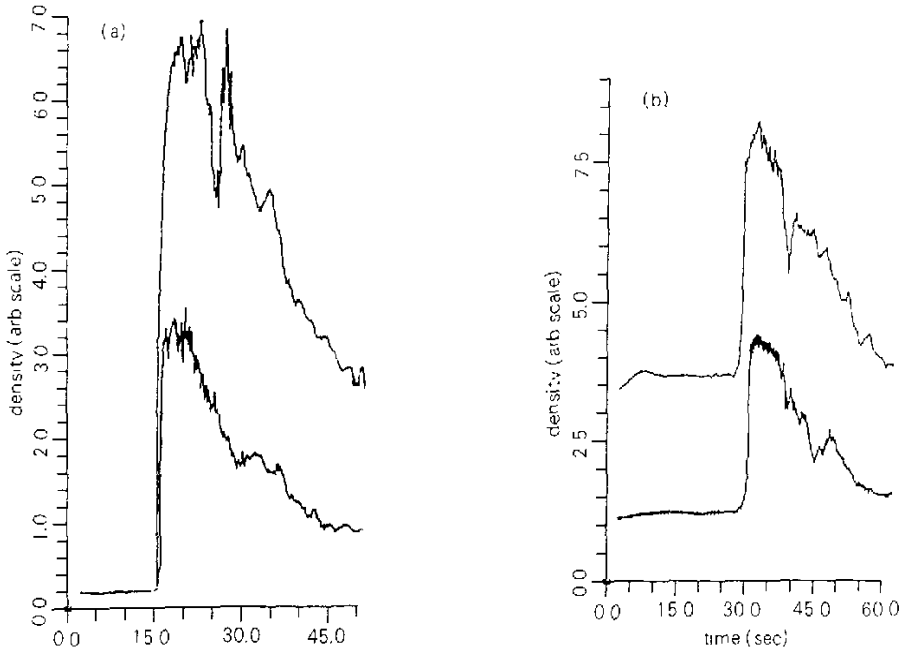

Fig. 10. Salinity signals from two probes, located at different levels with topographic effect: (a) without bottom slope and stratification and (b) without bottom slope, but with stratification ($Fr=0.8$).

the break up of the current head and its wake (in this case $Fr=0.8$).

Finally, in the third set of experiments (Fig. 11) a downslope floor from the place where the gravity current was released was placed in the channel. The slope of the floor was about 15°, extending to the edge where the topography started, about 80 cm downstream from the beginning of the channel. In such a case, the velocity of the current may be given by the equation (2) (Beghin et al., 1981). An interesting feature in these experiments is the increase in the number of dominant peaks behind the head, especially in the case without the effect of near surface stability. In a particular case (Figure 11b), the probes were placed at the interface between the two layers, 50 cm apart horizontally. Regular internal waves, with little irregular turbulence are evident in the signals.

Figures 9 and 11b show the signals for the first and third experimental set-ups, indicating the turbulence is effectively filtered, and only the main head and the dominant eddies behind the head produce bore like undulation in the signal. The wavy nature of the flow is particularly brought out, when the mean signal is subtracted from the original. Fig. 12a shows such a signal for the case with stratification. Its power spectral density is shown in Fig. 12b. Such behavior has been observed by Manasseh and Middleton (1995) and attributed to boundary layer oscillations.

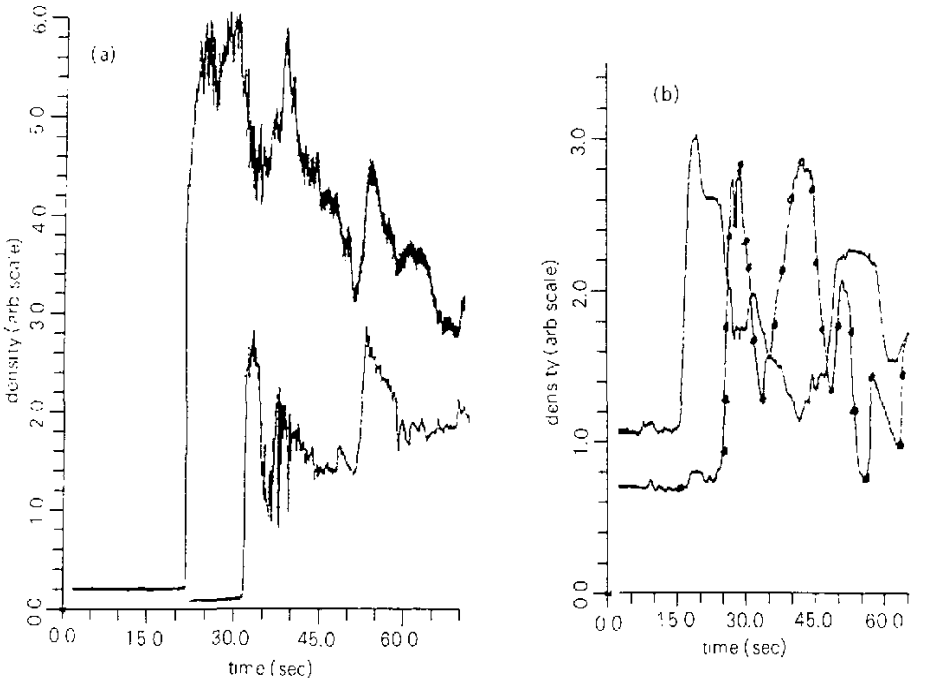

Fig. 11. Same as Fig. 10, but with bottom slope and probes placed at the same level while at different distance along the channel (about 85 cm apart): (a) without stratification ($Fr=0.71$), (b) with stratification ($Fr=0.78$).

Table 2 summarizes the characteristics of the density signal structures, including the Fr. The effect of near bottm stratification is to suppress lobes and cliffs instabilities and the gravity current time span (the time for the current to pass the probe) is reduced by about 10–15%. The time span of the current (and also the number of its main peaks) also increases with topography and sloped boundary effects. This is due to broadening of the current as topography spreads the structure of the gravity current. All these effects are responsible for the variations observed in the gust fronts, apart from the effects of their sources. The Froude number of the current is also reduced by topographic effect.

Table 2. Summary of the density signal structures of the gravity currents shown

Figure	Time span of the head (sec)	Total time span (sec)	Fr
8	5	30	0.9
9	5	25	0.85
10(a)	9	33	0.78
10(b)	10	28	0.8
11(a)	10	49	0.71
11(b)	10	45	0.78

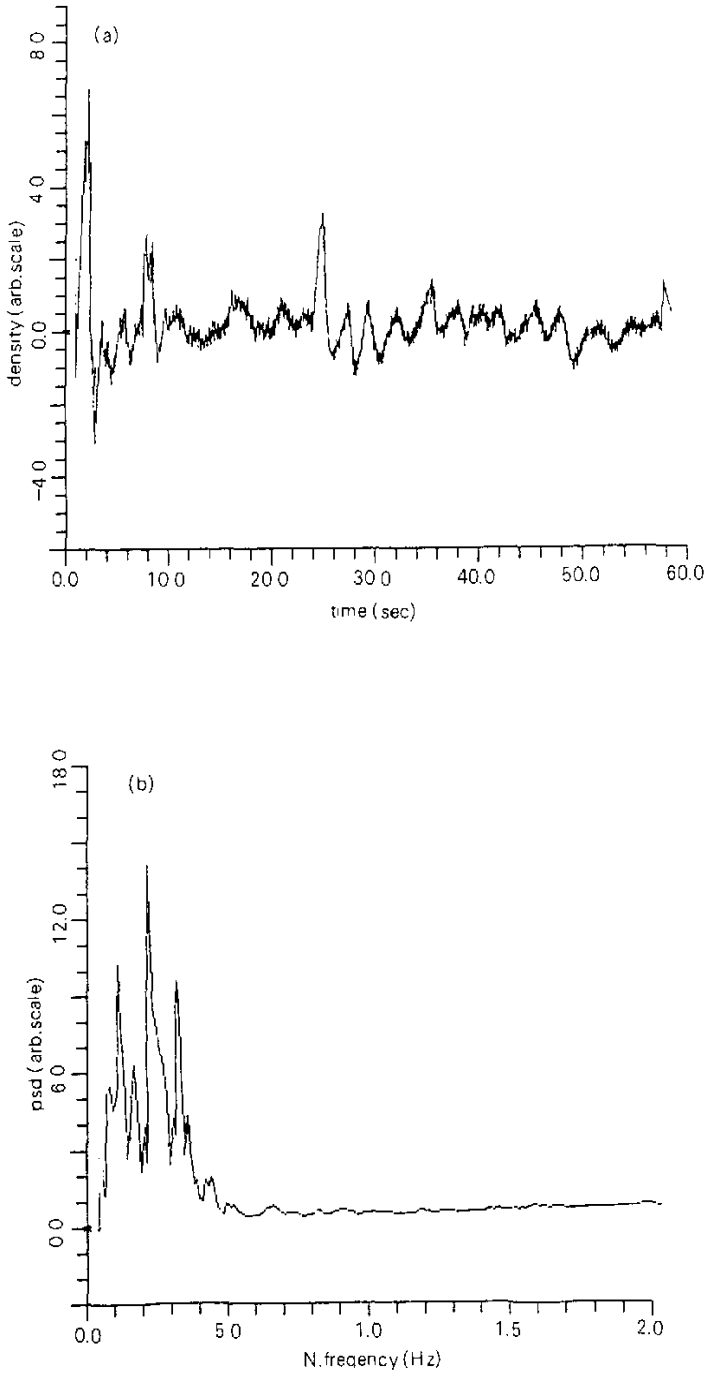

Fig. 12. (a) The fluctuating part of the signal shown in Fig. 9, and (b) its power spectral density ($Fr=0.85$).

5. Summary and discussion

Gust fronts originated from nearby thunderstorms mainly in Tehran area were studied, using surface meteorological observations. The gust front signals, particularly those of the wind speed, indicate that it has a clear head with a turbulent wake. The dominant peaks, behind the main one, which is due to the head, can be attributed to the organized advective cells at the top of the upper boundary. They may be due to the K–H instability, internal gravity waves (Weckwerth and Wakimoto, 1992) due to the topographic effects, which may also act as a cavity, generating vortices (Rangbar, 1997).

The gust fronts appear in different sizes and shapes, according to either their life-cycle stages or their origins. These variations may also be due to the effect of surface topography and ground slope. The Froude number varies between 0.8–1.4 and appears to be reduced by the increase in terrain roughness. The thickness of the head of the front varies from 1 to 2 km. The surface roughness in urban area can reduce the kinetic energy of the gust fronts substantially.

Table 3 shows dynamical properties of two gust fronts in Tehran area. Here, the frontal vertical speeds were calculated from continuity equation. Calculated and observed speeds of the current appear to be in agreement. Urban roughness also appears to increase mixing and hence the dissipation of the kinetic energy of the front (Fig. 5) and may lead to thicker gust front (e.g. for Shemiran in Table 3).

Table 3. Dynamical properties of two gust fronts

Frontal vertical speed (m / s)	Non-hydrostatic pressure (hPa)	Calculated horiz. wind speed (kt)	Max. observed velocity (mean) (kt)	Flow thickness (km)	Station	Date
4.0	1.8	32.0	45 (35)	1	Mehrabad	24-5-1991
5.0	1.2	34.0	40 (28)	1.0	Geophysics	24-5-1991
5.0	1.7	35.0	36(30)	1.1	Shemiran	24-5-1991
4.0	0.3	30	20(18)	1.7	Mehrabad	27-5-1995
2.0	0.6	29.0	33(20)	1.5	Geophysics	27-5-1995
6.2	0.15	24.0	13(10)	2.35	Shemiran	27-5-1995

The results of simulations clarify some features about the structure of the gust fronts. Direct observations and salinity signals reveal that the current can be broken by topography. However, the restrictions imposed by the side walls, including the topographic features, which have some consequences on the laboratory simulation, have certainly no counterparts in the actual gust fronts.

Generally, three sets of experiments were carried out in order to simulate the gust fronts with and without the effects of topography, sloping floor and bottom stability (near surface inversion). The gravity current has a distinctive head, followed by a turbulent wake and coherent, roll like eddy structures atop the body of the current. This is reflected in the salinity signals, surprisingly similar to the velocity signal of the gust fronts (Fig. 4). When the environment is stratified, such flows lead to wave like structures, which may have implications for low flying aircraft (Manasseh and Middleton, 1995). Topographic effect, which disintegrates the gravity current head, appears to reduce the Froude number of the flow. Also, the time span of the current appears to be increased as a result. It sometimes appears that a strong gust

front from one direction (e.g. north–west for Tehran) leads to a secondary thunderstorm downstream, which can in turn lead to the generation of gust fronts moving in opposite direction as in Fig. 2 (from southeast for Tehran). A remote sensing system such as a lidar is required to reveal vertical structure of the gust fronts for mountainous region as Tehran and this is being pursued.

As the gust fronts lift the warm (and may be moist) air ahead of them, that can feed the main thunderstorm, it might be a good idea to spread some proper cloud seeding materials in the air ahead of the front. Hence, by this mechanism, one may modify the thunderstorm behavior through its own dynamics. Seeding thunderstorm for flood and hail suppression is a way to reduce their destructions.

We thank the financial support of Tehran University for this work.

REFERENCES

Banta, R. M., and C. B. Schaaf, 1986: Thunderstorm genesis zones in the Colorado Rockey Mountains as determined by tracebase of geosynchronous satellite images. *Mon. Wea. Rev.*, **111**, 463–476.

Beghin, P., E.H. Hopfinger, and R. Britter, 1981: Gravitational convection from instantaneous sources on inclined boundaries. *J. Fluid Mech.*, **107**, 407–422.

Bowen, B.M., 1996: Example of reduced turbulence during thunderstorm outflows. *J. App. Met.*, **35**, 1028–1032.

Britter, R.E., and J. E. Simpson, 1981: A note on the structure of the head of an intrusive gravity current. *J. Fluid Mech.*, **112**, 459–466.

Goff, R.C., 1976: Vertical structure of thunderstorm outflows. *Mon. Wea. Rev.*, **104**, 1429–1440.

Mahoney, W.P. 1988: Gust front characteristics and the kinematics associated with interacting thunderstorm outflow. *Mon. Wea. Rev.*, **116**, 1474–1492.

Manasseh, R., and J. H. Middleton, 1995: Boundary oscillations from thunderstorm at Sydney airport. *Mon Wea. Rev.* **123**, 1167–1177.

Muller, C.K., and R. E. Carbone, 1986. Dynamics of thunderstorm outflow. *J. Atmos. Sci.*, **44**, 1878–1898.

Rangbar, A., 1997: Study and physical simulations of thunderstorm gust fronts. M. Sc. Thesis, Institute of Geophysics, Tehran University.

Simpson, J.E., 1986: *Gravity Currents in Environment and the Laboratory*. John Wiley & Sons, 244 pp

Wakimoto, R.M., 1982, The life cycle of thunderstorm gust front. *Mon. Wea. Rev.*, **110**, 1060–1082.

Weckwerth, T.M., and R. M. Wakimoto, 1992: The initiation and organization of convective cells atop a cold air outflow boundary. *Mon. Wea. Rev.*, **120**, 2169–2187.